JOURNAL OF THERMOPHYSICS AND HEAT TRANSFER
Vol. 24, No. 2, April–June 2010

Assessment of Collisional-Energy-Based Models for Atmospheric Species Reactions in Hypersonic Flows

Michael A. Gallis,* Ryan B. Bond,† and John R. Torczynski‡
Sandia National Laboratories, Albuquerque, New Mexico 87185-0346

DOI: 10.2514/1.46267

A recently proposed set of direct simulation Monte Carlo chemical reaction models, based solely on the collisional energy and the vibrational energy levels of the species involved, is applied to calculate equilibrium and nonequilibrium chemical reaction rates for atmospheric reactions in hypersonic flows. The direct simulation Monte Carlo model predictions are in good agreement with Park's model, several theoretical models, and experimental measurements. Physically plausible modifications to some of the direct simulation Monte Carlo models are presented that improve agreement. The observed agreement provides strong evidence that modeling of chemical reactions based on collisional energy and vibrational energy levels provides an accurate method for predicting equilibrium and nonequilibrium chemical reaction rates.

Nomenclature

E_c	=	collisional energy, J
E_i	=	internal energy, J
E_t	=	translational energy, J
i	=	vibrational energy state (pure)
$K_{\mathrm{eq},r}$	=	equilibrium reaction constant (pure)
k	=	reaction rate, $\mathrm{m}^3\ \mathrm{molecule}^{-1}\ \mathrm{s}^{-1}$
k_B	=	Boltzmann constant, J/K
m	=	mass, kg
q	=	temperature exponent in Park's model (pure)
T	=	temperature, K
Z	=	nonequilibrium reaction-rate parameter (pure)
Z_i	=	vibrational relaxation number (pure)
z_v	=	vibrational partition function (pure)
Γ	=	gamma function (pure)
ε	=	symmetry parameter (pure)
ε_i	=	specific internal energy of mode i, $\mathrm{J\,kg}^{-1}$
ζ	=	degrees of freedom (pure)
Θ_d	=	characteristic dissociation temperature, K
Θ_v	=	characteristic vibrational temperature, K
ω	=	viscosity temperature exponent (pure)

Subscripts

a	=	activation
c	=	collision
d	=	dissociation
eq	=	equilibrium
i	=	internal energy mode
max	=	maximum
mol	=	molecule
R	=	reaction
r	=	reduced for mass, relative for speed
ref	=	reference
rot	=	rotational
t	=	total
tr	=	translational
vib	=	vibrational

Received 7 July 2009; revision received 22 October 2009; accepted for publication 14 December 2009.

*Principal Member of the Technical Staff, Microscale Science and Technology Department, P.O. Box 5800, Mail Stop 0346. Senior Member AIAA.

†Senior Member of the Technical Staff, Aerosciences Department, P.O. Box 5800, Mail Stop 0825. Member AIAA.

‡Distinguished Member of the Technical Staff, Microscale Science and Technology Department, P.O. Box 5800, Mail Stop 0346.

I. Introduction

HIGH-SPEED flight usually takes place at high altitudes and involves the formation of shock layers. Because the velocity is high and the density is low, these shock layers typically produce significant regions of thermal and chemical nonequilibrium in the flow downstream. The gas properties in these regions are determined by the relative concentrations and energies of the various chemical species that are present. Thus, accurate predictions of heat transfer to the vehicle and radiation from its vicinity require accurate models for chemical reaction rates under conditions of significant thermal and chemical nonequilibrium.

The difficulty of measuring reaction rates has hampered the development of models that can accurately predict chemical reaction rates under nonequilibrium conditions. Because of the scarcity of measurements and their large uncertainties, it is often difficult to identify the important mechanisms that influence reaction rates and to quantify the accuracy of models that predict reaction rates under nonequilibrium conditions. As a result, models for nonequilibrium reaction rates are frequently based solely on equilibrium chemical reaction data. Making nonequilibrium predictions based solely on equilibrium data can lead to unknown and potentially large errors.

Since the late 1950s, many theoretical and empirical attempts have been made to overcome this difficulty. Building on the work of Hammerling et al. [1], Treanor and Marrone [2] developed the coupled vibration–dissociation–vibration (CVDV) model to account for the coupling of vibrational relaxation and dissociation processes. According to the CVDV model, dissociation can occur with equal probability from any level and is proportional to the product of the population in that level and the rate of collision with molecules energetic enough to cause dissociation. Thus, the lag in vibrational excitation inhibits the rate of dissociation because of the lack of highly energetic molecules.

More recently, many theoretical and empirical models [3] have attempted to relate the nonequilibrium reaction rate to its equilibrium rate and the degree of vibrational excitation using the deviational factor $Z(T_{\mathrm{tr}}, T_{\mathrm{vib}})$:

$$k(T_{\mathrm{tr}}, T_{\mathrm{vib}}) = k(T)Z(T_{\mathrm{tr}}, T_{\mathrm{vib}}) \tag{1}$$

where the subscripts tr and vib denote the translational and vibrational energy modes, respectively. Some of these models use empirical or adjustable parameters that are estimated based on experimental data or quantum mechanical computations, and some require only microscopic information.

Using equilibrium reaction-rate data from a large number of experimental and flight observations, Park [4,5] developed a two-temperature model to represent nonequilibrium behavior. In Park's model, the influence of the vibrational temperature on a chemical reaction rate is accounted for by replacing the temperature in the equilibrium (Arrhenius) rate with a geometric average of the translational and vibrational temperatures:

$$T = T_{\mathrm{tr}}^{q} T_{\mathrm{vib}}^{1-q}, \qquad q = 0.5\text{–}0.7 \tag{2}$$

Since its introduction in the late 1980s, Park's model and a set of reaction rates derived from experimental data and compatible with his model have become the standard approach for treating nonequilibrium chemically reacting flows within the framework of the Navier–Stokes equations. Although it has some degree of empiricism [6,7], Park's method successfully reproduces most of the experimental radiation data available for velocities up to 10 km/s [4,5].

The most widely used numerical method for modeling nonequilibrium gas flows is Bird's direct simulation Monte Carlo (DSMC) method [8]. Bird [9] recently developed a new model within the DSMC framework to predict chemical reaction rates using only kinetic theory considerations, the energy content of the particular collision, and the vibrational energy levels of the chemical species involved [10]. More specifically, this model does not rely on macroscopic rate information or adjustable parameters and does not require the gas to be in equilibrium [9,10]. This feature is particularly important when considering situations in which the reaction rates are not known, such as NASA missions to hydrocarbon-dominated planetary atmospheres.

In this paper, equilibrium and nonequilibrium reaction rates determined using these new DSMC models are compared to values from Park's and other models and experimental data for atmospheric chemical reactions that occur in hypersonic flows. The aim of this work is to assess the ability of the new model to reproduce equilibrium and nonequilibrium reaction rates between atmospheric species.

II. DSMC Modeling of Gas Flows

DSMC uses a particulate, stochastic algorithm that simulates the physical situation described by the Boltzmann equation. The continuous velocity distribution function is approximated with a discrete number of computational molecules, or simulators [8]. Simulators move, reflect from walls, and collide with each other according to prescribed interaction laws and thereby represent the noncontinuum behavior of a dilute gas under the assumption of molecular chaos. Each simulator typically represents a large number of real molecules.

A fundamental distinguishing feature of DSMC is the temporal decoupling of molecular motion and collision. This decoupling is appropriate when the time over which each aspect is allowed to occur (i.e., the time step), is much smaller than the mean collisional time. During a time step, molecules move ballistically at their velocity without interacting with neighboring molecules. Between moves, pairs of molecules within each cell are selected to collide at the appropriate rate. During molecular collisions, conservation laws are satisfied and physical effects are realized at the molecular level. From a mathematical point of view, the motional and collisional phases mimic the processes described by the corresponding terms on the left and right sides of the Boltzmann equation, respectively. Following this logic, DSMC simulators can be considered as points in phase space. The motional phase changes their positions but leaves their velocities unchanged. The collisional phase changes their velocities but leaves their positions unchanged.

Ideally, molecular interactions can be described with the appropriate cross sections. However, because of the very large number of possible interactions and the lack of accurate cross sections for them, molecular interactions are usually described with idealized molecular-interaction and energy-exchange laws. Although complicated molecular potentials, such as Morse or Lennard–Jones molecular interactions [11] have been used in DSMC [8], simplified models, such as the variable-soft-sphere (VSS) [8] molecular interaction and the generalized Larsen–Borgnakke (GLB) model for energy exchange [8], are almost universally used in DSMC, because they provide a good balance between physical realism and computational efficiency. By capturing the main features of microscopic mechanisms, these models reproduce known macroscopic behavior without reducing computational efficiency.

Although originally based on arguments of physical plausibility, the DSMC algorithm has been theoretically shown to provide an exact solution to the Boltzmann equation in the limit of infinite simulators and vanishing discretization errors (time step and cell size) [12]. Furthermore, DSMC has been shown to reproduce the results of infinite-order Chapman–Enskog theory for the transport properties of a monatomic gas [13]. More important, DSMC predictions for the transport properties under equilibrium [13] and nonequilibrium [14] conditions are in very good agreement with analytical solutions of the Boltzmann equation.

In the absence of accurate, state-specific chemical reaction cross-sectional data, DSMC uses phenomenological models that capture the essential features of the microscopic mechanisms while maintaining its computational efficiency. In a fashion similar to the molecular models used to simulate collisional dynamics and energy exchange, DSMC chemistry models attempt to reproduce the main properties of the chemical reactions in a computationally efficient manner.

Although DSMC procedures model physical phenomena at the molecular level, some of the information used to develop molecular models comes from the macroscopic level. For example, the variable-hard-sphere (VHS) and VSS molecular models [8] for a particular species both use macroscopic information (namely, the temperature dependence of viscosity) to determine a microscopic quantity: namely, the energy-dependent collisional cross section. Following this rationale, Bird's total collisional energy (TCE) model [8], the first chemical reaction model proposed for DSMC, relies heavily on measured equilibrium reaction rates to determine parameters that the microscopic DSMC model uses to simulate chemical reactions. Thus, using an assumed form of the collisional cross section and the collisional frequency of a VHS or VSS gas, the TCE model can reproduce almost any given Arrhenius reaction rate, which can be considered as an advantage of these models. The TCE model was followed by multiple extensions of varying sophistication and complexity that have been reviewed and comparatively evaluated on many occasions [15–19].

Bird [8,9] proposed a new type of models that are based solely on properties of the colliding molecules and do not use measured reaction rates or adjustable parameters. The microscopic properties used in these models include the available collisional energy, dissociation energies, and quantized vibrational energy levels. The lack of adjustable parameters means that these models cannot be adjusted to reproduce a given reaction rate. Instead, the new model predicts the reaction rate. In harmony with the principles of the CVDV model, the DSMC models link the chemical reaction process to the energy content of the vibrational state of the colliding molecules. Application of chemical reaction procedures for collisions between molecules that could lead to endothermic reactions is conceptually straightforward. The models for these forward endothermic reactions and the principle of microscopic reversibility are then used to develop models for the corresponding reverse exothermic reactions. These models satisfy microscopic reversibility by balancing the fluxes into and out of each state and do not require any macroscopic rate information.

In addition to their conceptual simplicity, the main advantage of these models is that they do not rely on macroscopic, experimentally measured reaction-rate data. The dissociation, recombination, and exchange-reaction cross sections are based on kinetic theory and vibrational-energy-level information. The fact that these models are implemented in an inherently nonequilibrium method, such as DSMC, suggests that nonequilibrium chemical reaction rates can be calculated with reasonable accuracy. This feature of the new models can be particularly important in cases in which the equilibrium reaction rates are not known.

A. Dissociation and Recombination Reactions

The introduction of quantum vibrational states in DSMC procedures [8] proved to be a significant step forward, because it allowed a more realistic representation of the energy in the lower widely spaced vibrational energy levels. The next step was to link the vibrational excitation to dissociation. Bird [8] suggested that dissociation reactions are part of the process of energy exchange between the colliding molecules. In this view, the exchange of vibrational energy is incomplete and inconsistent without linking it to dissociation and allowing collisions to populate vibrational states above the dissociation level. This concept is captured in an energy-threshold model proposed by Bird [8]. According to this model, during the energy-exchange process of a diatomic molecule, if the energy content of the vibrational mode exceeds the energy threshold of the dissociation or exchange reaction, the reaction occurs.

However, a continuum (i.e., an infinite number of states) exists above the dissociation limit [20]. Thus, a vibrational level above the dissociation level cannot be occupied or physically defined. Therefore, during a collision, if a dissociation reaction is energetically possible, it occurs. During the energy-exchange process in a collision between two simulators, where at least one of them is a molecule, energy $E_c = E_{\text{trans,pair}} + E_{\text{vib,mol}}$ would be made available to the vibrational mode, where $E_{\text{trans,pair}}$ is the translational energy of the pair and $E_{\text{vib,mol}}$ is the vibrational energy of the molecule in question. Assuming a harmonic oscillator model for the vibrational mode, the maximum vibrational level that could be obtained is $i_{\max} = \text{int}[E_c/k_B\Theta_v]$, where Θ_v is the characteristic vibrational temperature and k_B is the Boltzmann constant. If this level is higher than the dissociation level $i_d = \Theta_d/\Theta_v$, where Θ_d is the characteristic dissociation temperature, the reaction occurs. Assuming equilibrium at temperature T, the dissociation rate can be analytically calculated as

$$k(T) = \frac{2\sigma_{\text{ref}}}{\varepsilon\sqrt{\pi}}\left(\frac{T}{T_{\text{ref}}}\right)^{1-\omega}\left(\frac{2k_BT_{\text{ref}}}{m_r}\right)^{1/2} \times \left\{\sum_{i=0}^{i_d} Q\left[\frac{5}{2}-\omega, \frac{\Theta_d-(i-1)\Theta_v}{T}\right]\frac{\exp[-i\Theta_v/T]}{z_{\text{vib}}(T)} + B\sum_{i=i_d+1}^{\infty}\frac{\exp[-i\Theta_v/T]}{z_{\text{vib}}(T)}\right\} \tag{3}$$

where

$$Q\left[\frac{5}{2}-\omega, \frac{\Theta_d-(i-1)\Theta_v}{T}\right] = \frac{\Gamma\left[\frac{5}{2}-\omega, \frac{\Theta_d-i\Theta_v}{T}\right]}{\Gamma\left(\frac{5}{2}-\omega\right)}$$

is the probability of the translational energy exceeding the difference between the level i and the dissociation level i_d;

$$z_{\text{vib}} = (1-\exp[-\Theta_v/T])^{-1}$$

is the vibrational partition function in the harmonic oscillator model; σ, ω, and m_r are the collisional cross section, viscosity temperature exponent, and reduced mass of the pair, respectively; and ε is a symmetry parameter that is set to 1 for like molecules and to 2 for unlike molecules. The parameter B takes the values of 0 or 1, depending on whether the harmonic oscillator model for the vibrational states is truncated at the dissociation level or is not truncated. Although formulated for a VHS or VSS gas, Eq. (3) can readily be extended to any molecular model if the relevant collisional frequency replaces the first three terms of Eq. (3).

The TCE model considers the total collisional energy as the primary controlling parameter in determining the reaction probability and thus incorporates no selectivity in the energy dependence of chemical reactions. In contradistinction, the new model emphasizes the role of the vibrational energy in promoting a reaction by considering only the precollisional translational and vibrational energy as the energy that could be channeled in the postcollisional vibrational mode as the controlling parameter. This choice of participating energy modes is a reflection of the energy-exchange process that populates the vibrational mode. The choice of the translational and vibrational energy modes as the participating modes is also in agreement with the underlying GLB model that selects the vibrational energy of a molecule after a collision from the combined precollisional translational–vibrational energy pool. Effectively, excluding the rotational energy from consideration produces a form of selectivity of vibrational energy for promoting dissociation reactions.

The new DSMC model implicitly accounts for the effect of rotational energy participating in the dissociation process. It is known [3] that high-rotational energies can stimulate dissociation both by reducing the dissociation energy threshold via the centrifugal effect and by affecting the dynamics of collisions between rapidly rotating molecules. However, the relaxation times for energy exchange between the translational and vibrational modes are about 10^4 times longer than the relaxation times for energy exchange between the translational and rotational modes. Thus, during the time it takes for energy exchange between the vibrational and the translational mode, the translational and rotational modes come into equilibrium with each other. Because of the rapid equilibration of the rotational and translational modes, the rotational energy does not need to be included in the participating energy modes, because it effectively participates in the process through the translational energy. Directly including the rotational mode in the energy controlling the reaction would make the DSMC model lose its selectivity in the energy promoting a reaction.

Recombination requires a three-body collision. A three-body collision is considered to occur if a third simulator is found within a sphere whose radius is the interaction range of the colliding pair. Herein, the sum of the radii of the colliding atoms is taken to be the interaction range of the colliding pair, a choice in harmony with the assumptions of the VSS collisional model used for this work. The ratio of the collisional volume to the cell volume per simulator gives the probability that a simulator is found inside the collisional volume and therefore is the three-body collisional probability. Recombination occurs in a three-body collision between the appropriate atoms if the potentially recombined molecule after a trial energy redistribution of the relative translational energy of the atom–atom pair is found to be at the ground vibrational state. The addition of the dissociation energy to the vibrational mode of the newly formed molecule would then bring it to the state appropriate for dissociation. In this way, microscopic reversibility is satisfied.

B. Endothermic and Exothermic Exchange Reactions

According to Bird's model, endothermic exchange reactions take place when the vibrational level of the colliding molecule, after a trial energy-exchange redistribution of the collisional energy E_c, is one level above the level corresponding to the activation energy E_a:

$$i_a = \text{int}[E_a/k_B\Theta_v] + 1 \tag{4}$$

where i_a is the first vibrational level above the energy threshold of the reaction. The macroscopic rate at which this process occurs can be derived is

$$k(T) = \frac{2\sigma_{\text{ref}}}{\varepsilon\sqrt{\pi}}\left(\frac{T}{T_{\text{ref}}}\right)^{1-\omega}\left(\frac{2k_BT_{\text{ref}}}{m_r}\right)^{1/2}\frac{\exp[-i_a\Theta_v/T]}{z_{\text{vib}}(T)} \tag{5}$$

Bird suggests [9] that the reverse exothermic exchange reactions occur when the newly formed molecule after a trial energy redistribution of the total collisional energy, including the reaction energy E_a, is formed at the vibrational state corresponding to the activation energy, as in Eq. (4).

III. Equilibrium Rates for Atmospheric Reactions

Park's suggested reaction-rate set is currently the most commonly used set of reaction rates for calculating chemical reactions in atmospheric hypersonic flows. Because Park's model is based on equilibrium conditions, the DSMC models are compared to Park's

model for equilibrium conditions as a first step in assessing their accuracy.

When comparing reaction rates, two issues must be kept in mind. The first is the temperature range within which Park's model is appropriate. Most of the experimental data on which Park's reaction-rate set is based were obtained at temperatures below 10,000 K. For hypersonic flows, where the temperature reaches a value of 30,000 K, Park [4] suggests that the vibrational temperature should be limited to about 7000 K, resulting in a geometric-average temperature of 15,000 K. Through a series of comparisons with flight data, Park also suggests that the measured reaction rates can be safely extrapolated up to 30,000 K . The second has to do with the accuracy of these rates. Because of the variety of measurement techniques and methodologies used to infer these rates, the accuracy of the measurements cannot be easily determined. Few of the measured reaction rates have error estimations. Even for those that do, the problem becomes even more difficult in the temperature range in which these rates are extrapolated ($T \geq 10,000$ K). Park points out that some reaction rates measured for the same reaction differ by more than one order of magnitude; he suggests that his rates should be considered accurate only to within a factor of 3–10 [4].

Based on these observations and for the purpose of facilitating meaningful comparisons with DSMC rates, an uncertainty of one order of magnitude has been assigned to all measured and extrapolated rates presented herein. This uncertainty is designated by error bars in the relevant figures.

The DSMC chemistry models are implemented in a zero-dimensional DSMC code. Because the collisional phase in DSMC involves only simulators within a cell, unlike the motional phase, only a single cell need be considered. When two or more simulators are picked for collision, the probability of a chemical reaction occurring is calculated. To decide whether the chemical reaction would occur, this probability is compared to a random number uniformly distributed between 0 and 1. If the probability is greater than the random number, the number of reactions is advanced by one. However, unlike an actual simulation, the chemical reaction does not actually take place: the simulators are left unchanged. All the results presented herein are obtained using 10^6 simulators, with their properties sampled from the equilibrium distribution at the appropriate temperature. To enhance the statistical sample, and only for the equilibrium cases, molecules after a collision are allowed to redistribute their energy between the available modes.

In these single-cell tests, a single reaction is isolated and modeled. Thus, the mechanism of selecting between competing reaction rates does not need to be addressed within the context of these tests. Similarly, because the reactions are not realized, the problem of postreaction energy exchange is also not dealt with. These two problems need to be considered in a realistic flowfield simulation.

A. Dissociation Reactions

Atmospheric hypersonic flows are dominated by dissociation reactions of diatomic species: namely, nitrogen, oxygen, and nitric oxide. The first two of these occur naturally in the atmosphere, while the latter is produced at high temperatures. Because of its low energy threshold, the oxygen dissociation reaction has been the most thoroughly investigated, and therefore its rate is the most accurate. Nitrogen dissociation has a much higher energy threshold, which makes high-temperature experimental measurements more difficult. The nitric oxide dissociation reaction also has a low energy threshold. However, because of the highly efficient competing nitric-oxide formation and depletion exchange reactions, the dissociation rate is difficult to determine and thus less accurate.

Figures 1–3 present the dissociation reactions of O_2, N_2, and NO. In these figures, the dotted-dashed curves and solid circles represent the analytical expression: namely, Eq. (3) and the numerical implementation, respectively, of the DSMC model. The solid curves represent the reaction rates of Park's model. The agreement between the analytical expression and the numerical implementation verifies that the DSMC model has been correctly implemented. Based on the presumed accuracy of the measurements, the DSMC results are generally in good agreement with Park's rates. The DSMC predictions for oxygen and nitric oxide lie within the one-order-of-magnitude accuracy limit assumed for Park's rates, while the DSMC predictions for nitrogen lie at the edge of the accuracy limit. This

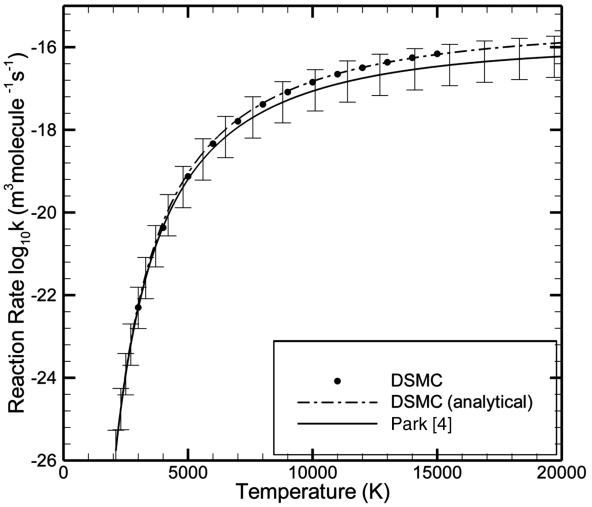

Fig. 1 Oxygen dissociation: $O_2 + O_2 \rightarrow O + O + O_2$.

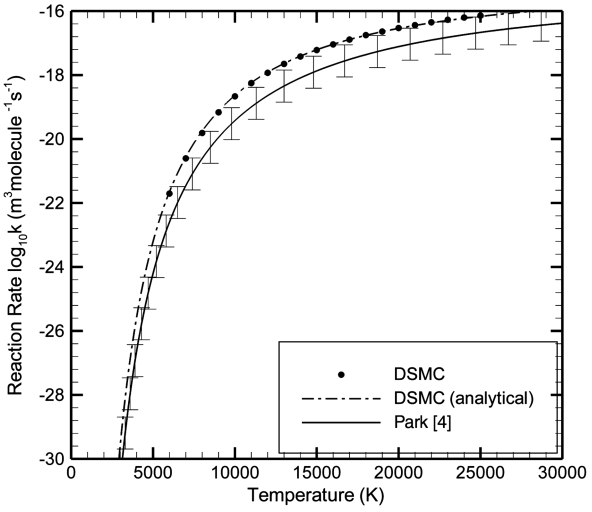

Fig. 2 Nitrogen dissociation: $N_2 + N_2 \rightarrow N + N + N_2$.

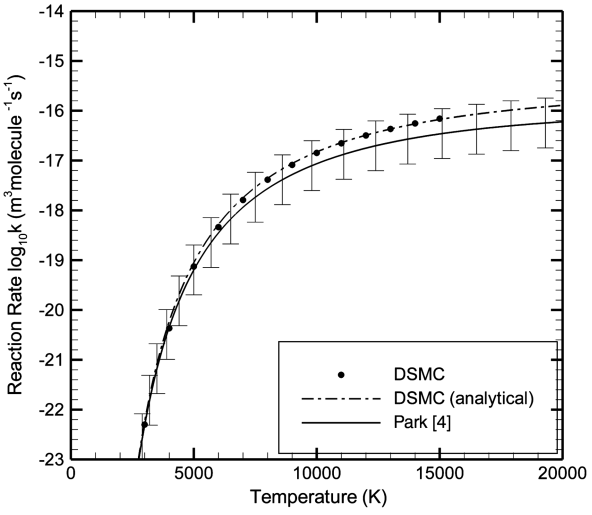

Fig. 3 Nitric oxide dissociation: $NO + NO \rightarrow N + O + NO$.

degree of agreement indicates that the DSMC model can predict dissociation reactions with reasonable accuracy.

B. Recombination Reactions

Recombination reactions are the reverse of dissociation reactions and are usually ignored in typical rarefied hypersonic applications due to their low probability of occurrence. The recombination reaction rate is based on the corresponding dissociation reaction rate and the equilibrium reaction constant $K_{\mathrm{eq},r}$. Park provides a method for calculating $K_{\mathrm{eq},r}$ as a function of the number density and temperature based on existing data for molecular constants augmented by solving the Schrödinger equation [4].

Figures 4 and 5 present the recombination reaction rates of atomic oxygen and atomic nitrogen as functions of temperature at equilibrium conditions. For this type of reaction, no analytical representation of the DSMC model is available. Thus, the DSMC model rates from the numerical implementation are compared to Park's recombination reaction rates. For oxygen, the DSMC recombination rate is in very good agreement with Park's rate. This agreement suggests that the DSMC model is accurate, because, as pointed out earlier, the oxygen rates are usually the most accurate. A larger difference, but still only marginally greater than the presumed order-of-magnitude accuracy limit of the measured rates, is observed for nitrogen recombination at high temperatures. Two explanations for this greater difference are possible. First, the difference could be attributed to the difference between the DSMC and Park nitrogen dissociation rates in Fig. 2, because the dissociation rate of Park is used to determine the recombination rate of Park in Fig. 5. Second, the difference could be attributed to a small inaccuracy of Park's fit of the equilibrium reaction constant at high temperatures, as observed by Gupta et al. [7].

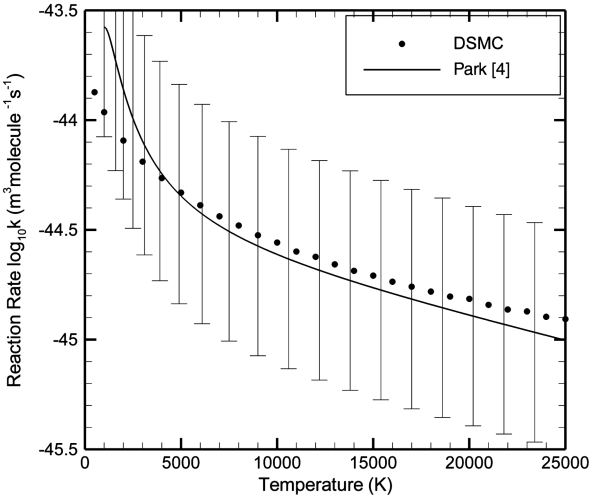

Fig. 4 Atomic oxygen recombination: $O + O + O \rightarrow O_2 + O$.

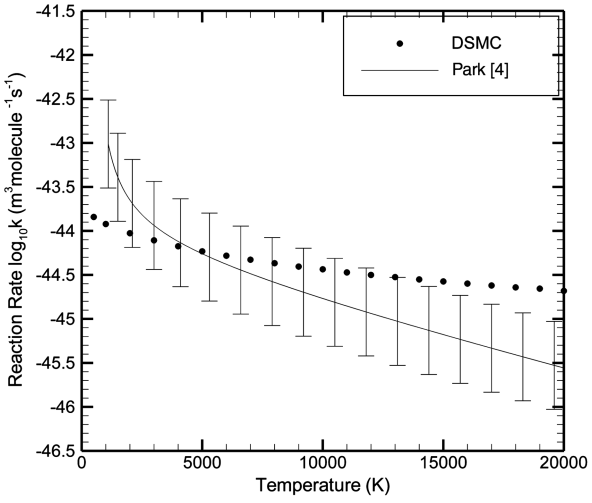

Fig. 5 Atomic nitrogen recombination: $N + N + N \rightarrow N_2 + N$.

C. Endothermic Exchange Reactions

Modeling exchange reactions is critical for simulating atmospheric hypersonic flows. Because of their low energy thresholds, exchange reactions are mainly responsible for the formation and depletion of nitric oxide, which is a major radiating species in atmospheric hypersonic flows. The two most important endothermic reactions taking place in atmospheric hypersonic flows are the following:

$$N_2 + O \rightarrow NO + N \tag{6}$$

$$NO + O \rightarrow O_2 + N \tag{7}$$

Figures 6 and 7 present the reaction rates of the endothermic exchange reactions of Eqs. (6) and (7), respectively. As observed for dissociation reactions, the agreement between the analytical expression and the numerical implementation verifies that the model has been correctly implemented in the DSMC code. For the first reaction $N_2 + O \rightarrow NO + N$, as shown in Fig. 6, the DSMC rates are

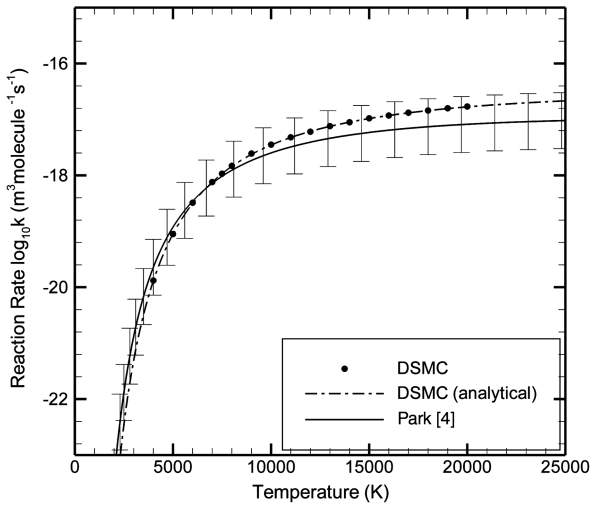

Fig. 6 Nitrogen/atomic-oxygen endothermic exchange reaction: $N_2 + O \rightarrow NO + N$.

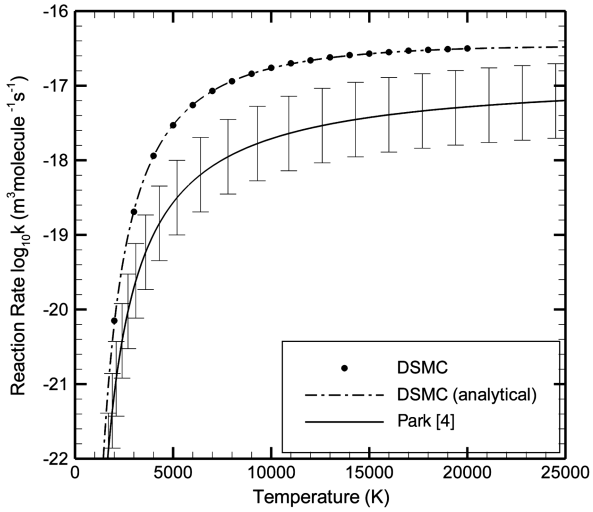

Fig. 7 Nitric-oxide/atomic-oxygen endothermic exchange reaction: $NO + O \rightarrow O_2 + N$.

in good agreement with Park's rates. A greater difference is observed between the DSMC rates and Park's rates for the second reaction $NO + O \rightarrow O_2 + N$, as shown in Fig. 7, especially at high temperatures. Because these reaction rates have been measured only at relatively low temperatures, below 5000 K, their values and accuracy are uncertain at temperatures approaching 15,000 K.

Monat et al. [21] provided measurements for the rate of the reaction $N_2 + O \rightarrow NO + N$ of Eq. (6) in the temperature range of 2384–3850 K. The quoted uncertainty is 35%, and other measurements are all within a factor of 3, so this reaction rate is one of the best known [4]. The DSMC rate in the temperature range of the experiment differs by only 50% from the measured value, a difference marginally outside the quoted measurement error. Park's suggested rate over the same temperature difference has an average difference of only 15% from the measured rate.

D. Exothermic Exchange Reactions

Exothermic exchange reactions are the reverse reactions of forward endothermic exchange reactions. No direct measurements for these reverse reactions exist, so their reaction rates are determined from the equilibrium reaction constants and the corresponding forward reaction rates. The exothermic exchange reactions $NO + N \rightarrow N_2 + O$ and $O_2 + N \rightarrow NO + O$ are the reverse reactions of the forward reactions in Eqs. (6) and (7), respectively, and are considered here.

Figures 8 and 9 present the DSMC and Park rates for these two reactions, respectively. In both figures, the solid symbols represent the DSMC rates, and the solid curves represent Park's rates. For the $NO + N \rightarrow N_2 + O$ reaction, the two rates are in good agreement only for temperatures around 10,000 K, where the two curves intersect, and have different trends with temperature. More specifically, the DSMC rate gradually increases up to 5000–10,000 K and appears to plateau at higher temperatures, whereas Park's rate peaks at about 1000 K and decreases from that point on. Nevertheless, if Park's reaction rates are taken to be accurate only to within one order of magnitude, the DSMC model is actually in fairly good quantitative agreement with Park's rates over the temperature range of interest. For the $O_2 + N \rightarrow NO + O$ reaction, the DSMC rates are in reasonable agreement with Park's rates. As for the $NO + N \rightarrow N_2 + O$ reaction, the DSMC rates appear to plateau above 10,000 K, whereas Park's rates decrease very slowly above 5000 K.

The concerns about the accuracy of the forward exchange reaction rates also apply to the reverse reaction rates because the forward reaction rates are used to determine the reverse reaction rates. Therefore, it is difficult to assess the accuracy of the DSMC model unequivocally based on this degree of agreement with Park's model.

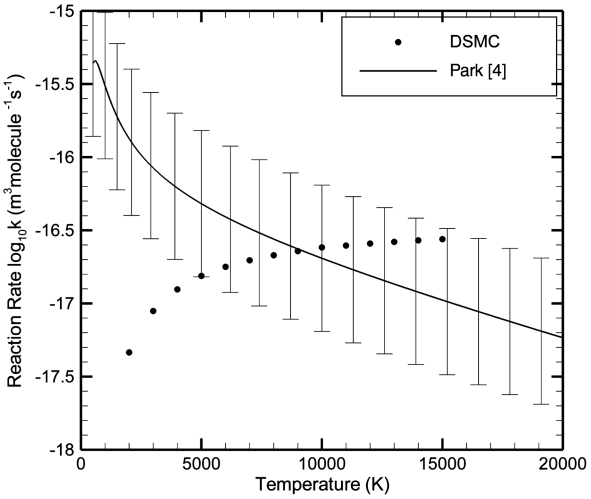

Fig. 8 Nitric-oxide/atomic-nitrogen exothermic exchange reaction: $NO + N \rightarrow N_2 + O$.

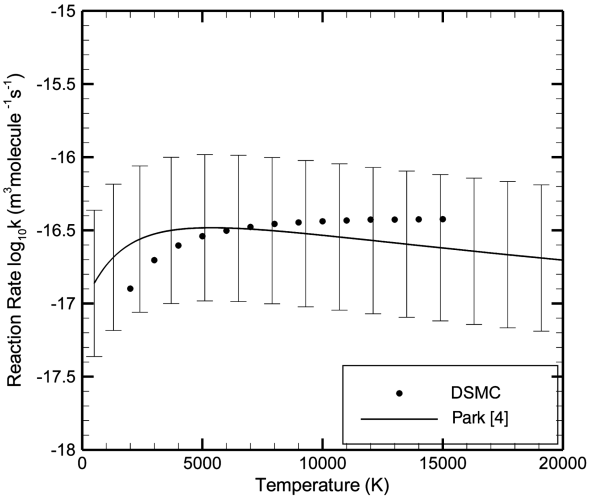

Fig. 9 Oxygen/atomic-nitrogen exothermic exchange reaction: $O_2 + N \rightarrow NO + O$.

The phenomenological mechanism for exothermic exchange reactions could also be formulated in a manner similar to that of recombination reactions. Thus, an energetically equivalent mechanism would require that the condition for the reverse exothermic exchange reaction to take place is that the potentially newly formed molecule after a trial GLB redistribution of the available relative translational and vibrational energy is in the ground vibrational state. Next, the energy released during the reaction is added to the vibrational mode to bring it to the state where the forward reaction is possible. Although the two schemes appear to be similar in terms of the final distribution of energy in the products, they result in different probability distributions for the reaction. This is due to the nonlinear dependence of the GLB distributions on the energy. However, both mechanisms produce reaction rates of the same order of magnitude. This indicates the ability of these phenomenological models to capture the correct order of magnitude of reaction rates, although the precise mechanism may not reproduce the details of the interaction exactly.

IV. Nonequilibrium Rates for Atmospheric Reactions

The ability of a chemistry model to reproduce equilibrium chemical reaction rates is a necessary condition to simulate chemically reacting flows. However, in atmospheric hypersonic flows, the chemical reactions take place under nonequilibrium conditions. Thus, the ability of any model to produce accurate chemical reaction rates under nonequilibrium conditions is particularly important.

Measured internal-energy-dependent cross sections of reactions between atmospheric species are extremely rare. Some systematic measurements and calculations exist for molecular hydrogen [15], where the cross section is found to be significantly affected by the distribution of energy among the reactant molecules. However, because of the relatively more important role of quantum effects in its interactions, the behavior of hydrogen is expected to deviate from the behavior of heavier and therefore more classical, atmospheric molecules.

In the absence of detailed state-specific information that can be used to validate models for nonequilibrium conditions, a comprehensive evaluation of any DSMC chemistry model is not possible. Therefore, the DSMC chemistry models are herein compared to nonequilibrium chemical reaction rates from approximate empirical and theoretical models. Although comparison with more established theoretical models cannot provide a validation of the DSMC model, it offers valuable insight into the performance of these models under nonequilibrium conditions.

In general, these models can be divided into two categories:

1) Empirical models, such as Park's model, estimate nonequilibrium effects based on experimental observations.

2) Theoretical models use approximate but physically realistic mechanisms to describe the role of vibrational energy in promoting chemical reactions.

Using the DSMC chemistry models, arbitrary nonequilibrium conditions can be simulated, and the effective reaction rate under nonequilibrium conditions can be calculated. Calculating nonequilibrium reaction rates with the DSMC models presented herein entails no differences in modeling because only collisional energy and vibrational-energy-level information is used.

The approach used to study nonequilibrium conditions is the same as that used to study equilibrium conditions, except that the vibrational temperature is prescribed independently from the temperature of the translational and rotational modes. Thus, the gas is characterized by two temperatures: T_{tr}, which describes the translational and rotational modes, and T_{vib}, which describes the vibrational mode. The energy states are distributed according to the Boltzmann distribution for the internal modes and the Maxwell distribution for the translational modes. To some degree, these conditions represent the state of a gas in a Navier–Stokes nonequilibrium calculation.

In the preceding section, the analytical expression and the numerical implementation of the DSMC models are compared to each other and to the measured reaction rates. The degree of agreement observed in these comparisons provides a verification and validation of the DSMC models.

For dissociation reactions and for the particular situation of the translational and vibrational energies being distributed according to their equilibrium distributions but at different translational and vibrational temperatures (T_{tr} and T_{vib}, respectively), the reaction rate can be analytically calculated as

$$k(T_{\text{tr}}, T_{\text{vib}}) = \frac{2\sigma_{\text{ref}}}{\varepsilon\sqrt{\pi}} \left(\frac{T_{\text{tr}}}{T_{\text{ref}}}\right)^{1-\omega} \left(\frac{2k_B T_{\text{ref}}}{m_r}\right)^{1/2} \times \left\{ \sum_{i=0}^{i_d} Q\left[\frac{5}{2} - \omega, \frac{\Theta_d - (i-1)\Theta_v}{T_{\text{tr}}}\right] \frac{\exp[-i\Theta_v/T_{\text{vib}}]}{z_{\text{vib}}(T_{\text{vib}})} + B \sum_{i=i_d}^{\infty} \frac{\exp[-i\Theta_v/T_{\text{vib}}]}{z_{\text{vib}}(T_{\text{vib}})} \right\} \tag{8}$$

Unlike the DSMC model for dissociation reactions, the DSMC model for exchange reactions considers postcollisional properties of the colliding molecules. While under conditions of equilibrium the postcollisional distribution of energy is known, it is not so for nonequilibrium conditions, which in fact requires a time-dependent solution. Thus, an analytical expression similar to that of Eq. (5) for exchange reactions cannot be derived under nonequilibrium conditions.

Figure 10 presents nonequilibrium reaction rates for oxygen dissociation as a function of the vibrational temperature at translational–rotational temperatures of 15,000, 10,000, 5000, and 3000 K. The vibrational energy is distributed according to the harmonic oscillator model at temperatures from 500–15,000 K. The values from Eq. (8) are designated by curves, whereas the numerically calculated values are designated by symbols. As observed for equilibrium conditions (see Figs. 1–3), the numerical values are in very good agreement with the analytical expression for nonequilibrium conditions, indicating that the DSMC model is correctly implemented.

Figure 11 presents the same oxygen dissociation rates in comparison with the measured Arrhenius rate of Park [4,5], where the temperature has been replaced by the kinetic theory definition of the average temperature T for nonequilibrium gases in which the translational temperature T_{tr}, the rotational temperature T_{rot}, and the vibrational temperature T_{vib} are interpreted as above in terms of the thermal energy in each of these modes, respectively:

$$T = \frac{3T_{\text{tr}} + \zeta_{\text{rot}} T_{\text{rot}} + \zeta_{\text{vib}} T_{\text{vib}}}{3 + \zeta_{\text{rot}} + \zeta_{\text{vib}}} \tag{9}$$

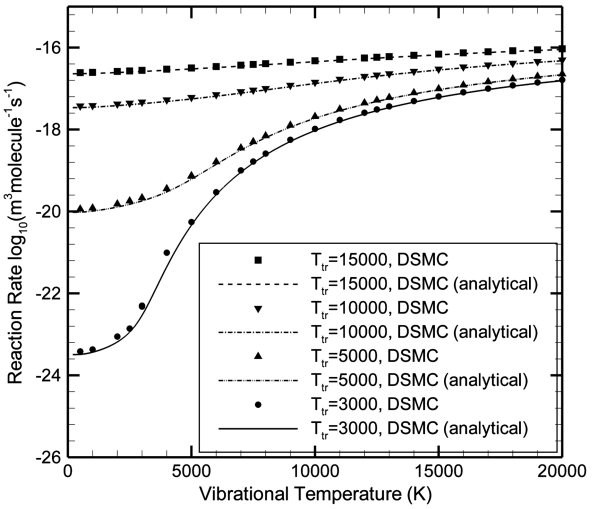

Fig. 10 Oxygen dissociation: DSMC numerical and analytical results for nonequilibrium conditions.

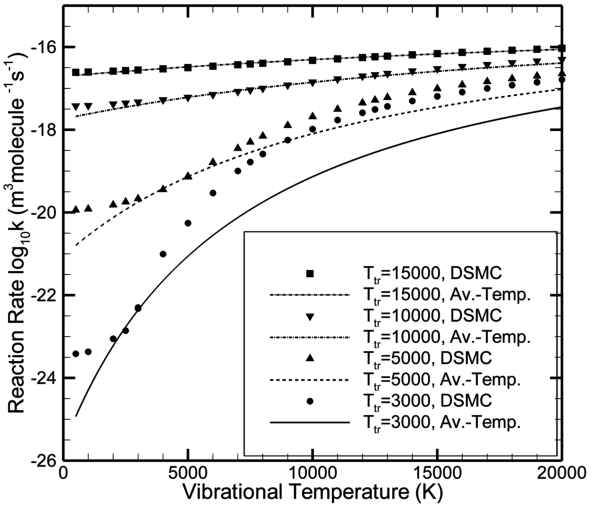

Fig. 11 Oxygen dissociation: DSMC and average-temperature rates.

In the above expression, the numbers of rotational and vibrational modes, ζ_{rot} and ζ_{vib}, respectively, are considered to be constant. Thus, Eq. (9) is an expression of the average temperature in terms of the average energy in all available energy modes.

With this interpretation of temperature as the average energy available in the colliding molecules, the Arrhenius rates can provide an estimate of the nonequilibrium reaction rate in the absence of any other information. This Arrhenius/average-temperature rate would be the prediction of the nonequilibrium reaction rate for any DSMC model that treats all three energy modes as equally likely to promote a reaction. Whereas the predictions for high temperatures are in good agreement, the predictions of the new model and the Arrhenius/average-temperature model are in disagreement for low vibrational temperatures. This difference in the behavior of the two models is an effect of the energy selectivity of the new DSMC model.

In agreement with theoretical predictions and experimental evidence [22], the new DSMC model predicts that the role of the vibrational energy in promoting a reaction varies with total energy for a particular reaction. The energy requirements of reactions become less restrictive at higher-collisional energies. At low-collisional energies, the selective energy requirements can significantly influence the reaction rate. This behavior has been commonly observed for the particular case of dissociation reactions, where higher vibrational temperatures become particularly effective in promoting dissociation reactions [15].

A. DSMC and Park's Model

Figures 12 and 13 present nonequilibrium reaction rates for nitrogen and oxygen dissociation at translational–rotational temperatures of 15,000, 10,000, 5000, and 3000 K. Park's rates with $q = 0.5$ are designated by curves, and DSMC rates are represented by solid symbols. In each case, the vibrational energy is distributed according to the harmonic oscillator model at temperatures from 500–15,000 K for oxygen and from 1000–17,500 K for nitrogen. The DSMC nonequilibrium reaction rates at vibrational temperatures above 10,000 K are relatively insensitive to the vibrational energy. A higher sensitivity is observed for lower vibrational and translational temperatures. The DSMC rates are in good agreement with Park's rates at translational temperatures above 10,000 K. However, a difference of several orders of magnitude is observed for vibrational temperatures below 5000 K. The rapid decrease of Park's rates with decreasing temperature in this range is explained by the dependence of the geometric-average temperature used in the Arrhenius rates on the vibrational temperature given by Eq. (2). In contradistinction, as pointed in the preceding section, the DSMC model allows the translational energy to participate in the energy used to overcome the energy barrier of the reaction. Thus, in the DSMC model, when the total energy is large enough, the sensitivity to the partition of energy diminishes. This behavior is in agreement with other theoretical and experimental observations [22].

Fitting the DSMC rates by Park's Arrhenius-rate type of equation and using the temperature in Eq. (2) with q as an adjustable parameter yields q values of 0.78 and 0.70 for oxygen and nitrogen, respectively. Figures 14 and 15 show the resulting rates for nitrogen and oxygen using these fittings, respectively. The nonequilibrium reaction rates using Park's model with the fitted values of q are in better agreement with the DSMC values, especially for temperatures less than 5000 K. This agrees with the suggestion of Sharma et al. [6] that a weaker dependence of the average temperature on the vibrational temperature (i.e., a larger q value of approximately 0.7) may be more accurate and that multitemperature effects on dissociation rates may be smaller than initially anticipated.

Figures 16 and 17 present the rates for the endothermic exchange reactions $N_2 + O \rightarrow NO + N$ and $NO + O \rightarrow O_2 + N$, respectively. The DSMC rates are in agreement with Park's rates for high-temperature conditions, although the difference in the lower-vibrational-temperature regime observed for dissociation reactions is observed here as well. The temperature regime in these figures is critical in modeling atmospheric hypersonic flows, because it represents the conditions behind a shock layer (high translational temperature, low vibrational temperature). In a typical high-altitude hypersonic flow, where the freestream vibrational temperature is initially negligible, the flow passes through the vibrational-temperature regime in the figure from left to right. Thus, a poor estimate

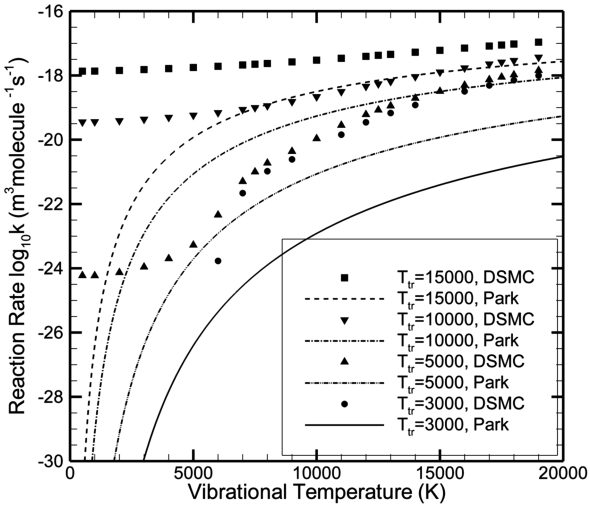

Fig. 12 Nitrogen dissociation: DSMC and Park's ($q = 0.5$) model.

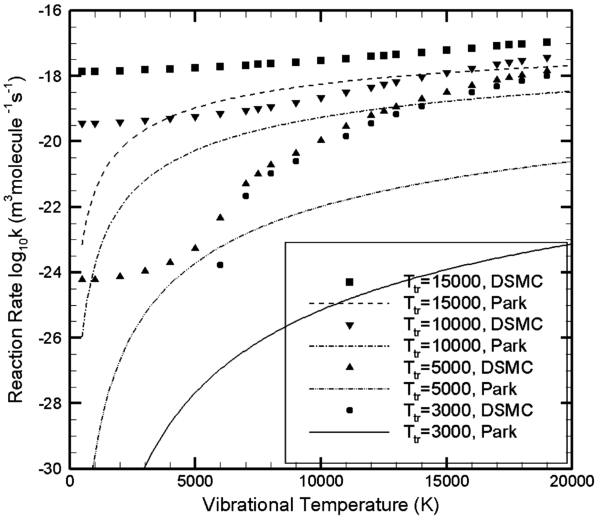

Fig. 14 Nitrogen dissociation: DSMC and Park's ($q = 0.70$) model.

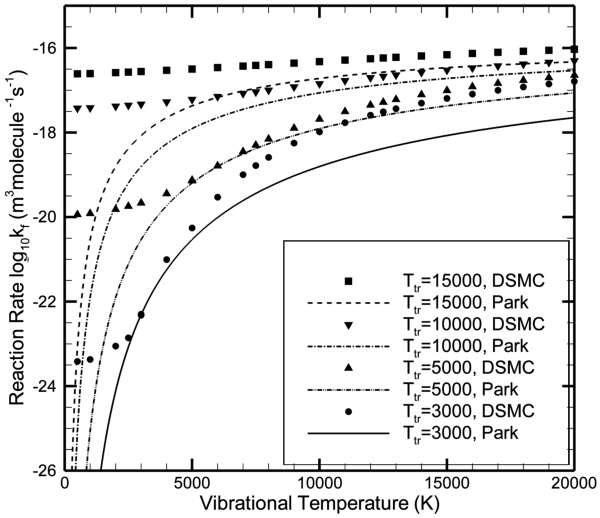

Fig. 13 Oxygen dissociation: DSMC and Park's ($q = 0.5$) model.

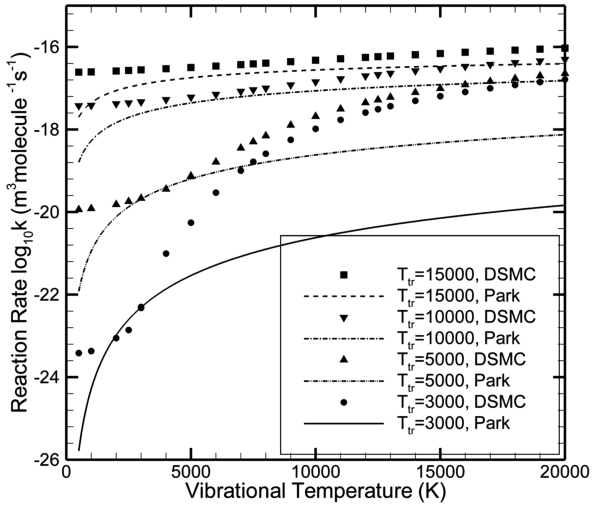

Fig. 15 Oxygen dissociation: DSMC and Park's ($q = 0.78$) model.

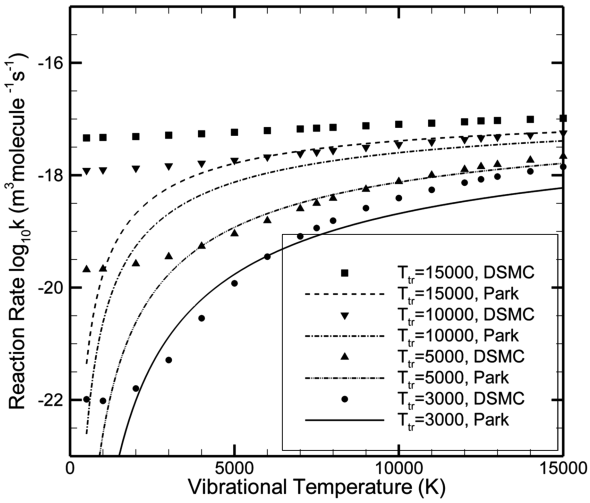

Fig. 16 $N_2 + O \rightarrow NO + N$ exchange reaction: DSMC and Park's model.

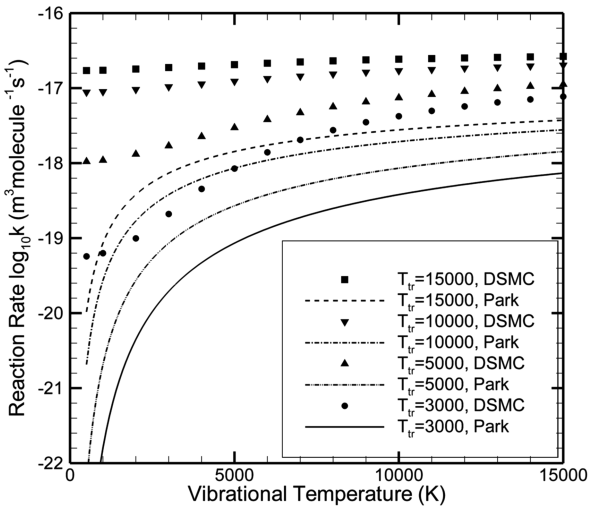

Fig. 17 $NO + O \rightarrow O_2 + N$ exchange reaction: DSMC and Park's model.

of the reaction rates in this initial temperature regime yields lower dissociation of oxygen. The dissociation of oxygen is usually the first reaction that takes place and is followed by the exchange reaction $N_2 + O \rightarrow NO + O$. Results based on underestimated oxygen dissociation reaction rates yield significantly lower (200 times) NO concentrations compared to flight measurements [23].

B. DSMC and Measured Rates

The differences between DSMC and Park's model at low temperatures cannot be resolved without measured data. Unfortunately, very limited data are available for atmospheric reaction rates under nonequilibrium conditions. Sergievskaya et al. [24] reported a small number of dissociation reaction rates obtained from shock-tube measurements that involve atmospheric species.

Figure 18 presents the upper and lower limits of measurements for oxygen dissociation reported by Sergievskaya et al. [24]. The vibrational temperature was kept constant at 4200 K, and the translational and rotational temperatures were kept in equilibrium with each other. The nonequilibrium rates are presented in terms of the deviational parameter Z of Eq. (1). Figure 18 also presents the ratio of the nonequilibrium to equilibrium reaction rates from the DSMC model and from Park's model using $q = 0.5$, as originally suggested by Park, and using $q = 0.78$, as calculated here by fitting Park's model to the DSMC values in accord with the suggestion of

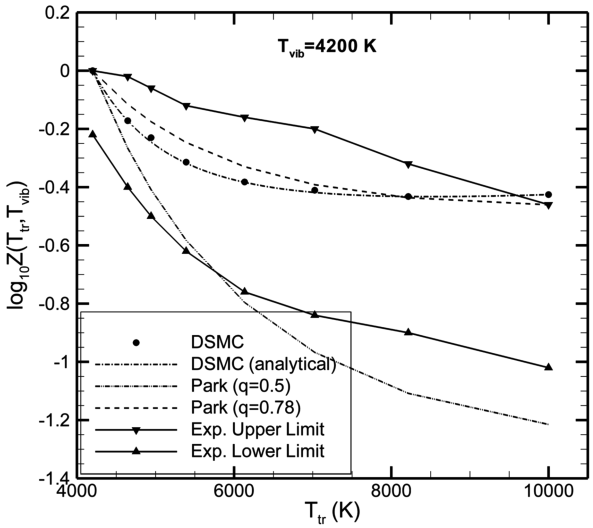

Fig. 18 Oxygen dissociation: DSMC and measured nonequilibrium rates.

Sharma et al. [6]. For a translational temperature of 4200 K, all model curves intersect. At this point, the gas is in thermal equilibrium, so the deviational parameter equals unity. As the translational temperature increases, the degree of nonequilibrium also increases. It is observed that the measured rates qualitatively reproduce the trend observed in the preceding section for highly nonequilibrium conditions, where the reaction rates reach a plateau as a function of the translational temperature.

Park's original model with $q = 0.5$ deviates from the measurements when nonequilibrium effects become appreciable. However, adopting a factor of $q = 0.78$ for Park's model brings its nonequilibrium values into good agreement with the DSMC values and the experimental measurements.

An indication of the measurement uncertainty is given by the underprediction of the equilibrium point, where upper bound of the measurements is at the expected value of unity but the lower bound is significantly different. As conditions depart from equilibrium, the DSMC rates are bounded by the experimental results, with the exception of the point at 10,000 K, where the DSMC model slightly overpredicts the experimental value. This overprediction is less than the uncertainty in the measurements near the equilibrium point and is much less than the difference between the lower and upper bounds at 10,000 K. Although not quite one order of magnitude, the spread in the experimental measurements is significant, so an unequivocal assessment of the models cannot be made.

C. DSMC and Theoretical Models

Significant effort has been expended in attempts to express the dependence of the reaction rate on the degree of vibrational excitation. Many empirical and theoretical models [3] have been proposed for the nonequilibrium deviational parameter $Z(T_{\mathrm{tr}}, T_{\mathrm{vib}})$ of Eq. (1). Some of these models use empirical or adjustable parameters that are estimated based on experimental data or quantum mechanical computations, and some require only microscopic information. The existing empirical and theoretical models for dissociation reactions are more advanced than those for exchange reactions. Both classes of models have been extensively reviewed in the literature [3,25].

Several theoretical models are used herein to assess the ability of the DSMC models to calculate nonequilibrium reaction rates. Because these models relate the nonequilibrium reaction rate to the equilibrium rate $k(T)$, the DSMC equilibrium rates are used in Eq. (1).

Figure 19 compares oxygen dissociation rates from the DSMC model and the adiabatic dissociation model (ADM) of Smekhov et al. (as discussed in Chernyi et al. [3]) for translational–rotational temperatures of 15,000, 10,000, 5000, and 3000 K. The ADM model

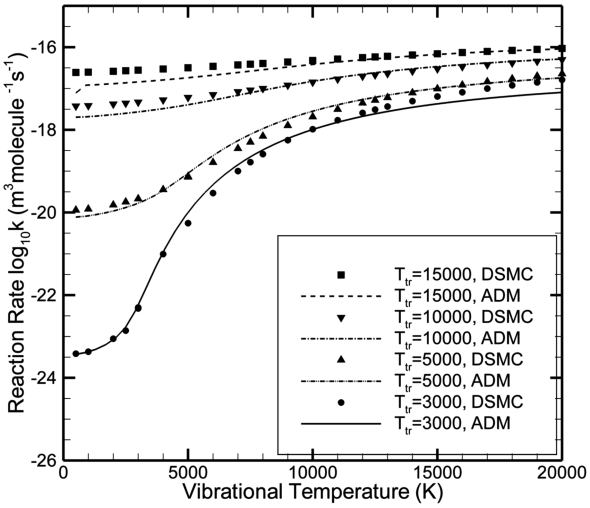

Fig. 19 Oxygen dissociation: DSMC and the ADM model.

is one of the most general models for dissociation reactions and is based entirely on theoretical considerations. The ADM model assumes that the energy states are distributed according to the Boltzmann distribution for the vibrational modes and the Maxwell distribution for the translational modes. The vibrational and translational modes are each characterized by single but distinct temperatures. The ADM model assumes that dissociation can occur from any vibrational level, including the ground state. However, the energy threshold is a function of the translational energy, which accounts for intramolecular energy transfer during a collision. The dissociation cross section is given by the Massey adiabatic parameter as $\sigma = \sigma_T \exp(-\xi)$, where σ_T is the total cross section and ξ is a function of the translational energy (Chernyi et al. [3]). The vibrational mode is described by the Morse anharmonic oscillator model. The DSMC rates are in excellent agreement with the ADM rates, especially for low temperatures. The slight degradation of agreement for higher temperatures can be attributed to the harmonic oscillator model used in the DSMC model to describe the vibrational mode.

Figure 20 presents a similar comparison for oxygen dissociation between the DSMC model and the Macheret–Fridman (M–F) model (Chernyi et al. [3]). The M–F model uses two distinct dissociation mechanisms, one from the lower vibrational levels and another from the upper vibrational levels. The translational energy plays a critical role for dissociation from the lower vibrational levels. Dissociation occurs only for particular relative configurations of colliding molecules that minimize the energy barrier. The M–F model produces deviations from the experimental data in excess of one order of magnitude [3], which may explain the significant differences observed here between the DSMC and M–F rates, especially in the low-vibrational-temperature regime.

Figure 21 presents oxygen dissociation rates from the DSMC model and the Treanor–Marrone (T–M) model [2]. The T–M model uses a truncated harmonic oscillator to describe the vibrational mode and assumes that dissociation can occur from any vibrational state without distorting the Boltzmann distribution of molecules over vibrational levels. The T–M model contains an adjustable parameter that is estimated by comparison with experimental data or quantum mechanical calculations. The value suggested by Chernyi et al. [3] is used here. According to Capitelli et al. [26], this adjustable parameter must depend on the translational temperature and on the vibrational level for the T–M model to agree with quantum mechanical calculations, and, even when these dependences are included, the T–M model underpredicts reaction rates for low vibrational temperatures. These observations may explain why the T–M rates lie below the DSMC rates in Fig. 21, especially at low temperatures. The differences between the ADM, M–F, T–M, and DSMC models are attributed to differences in how each model allows translational energy to promote dissociation reactions from low vibrational states.

These conclusions are not unique to oxygen dissociation. Results obtained for nitrogen dissociation are not presented here, because they are qualitatively similar to the results obtained for oxygen dissociation.

The DSMC model is in reasonable quantitative agreement with all of these theoretical models for high-collisional energies. Good agreement is also observed between the ADM model and the DSMC model for low vibrational temperatures, where the reaction rate is influenced mainly by the translational energy of the colliding pair. The qualitative agreement between the various models indicates that all of these models are predicting similar reaction energy selectivity. Unlike Park's model, the DSMC model and all theoretical models predict nonvanishing reaction rates as the vibrational temperature tends to zero. The large differences between the ADM, M–F, and T–M models in this limit may be taken as an indication of the uncertainty in these theoretical models. In the light of this, the qualitative agreement cannot lead to an unequivocal assessment of the accuracy of any of these models.

Figures 22 and 23 compare the DSMC model and the α model of Rusanov and Fridman (as discussed in Chernyi et al. [3]) for the endothermic exchange reactions of Eqs. (6) and (7), respectively. The α model assumes that only a fraction α of the vibrational energy participates in overcoming the energy threshold, whereas the translational energy is fully used in overcoming the energy threshold. The α model produces nonequilibrium reaction rates that are in very good agreement with DSMC nonequilibrium rates. This agreement cannot be considered a validation of either of the two models. The fraction α of the vibrational energy that participates in overcoming

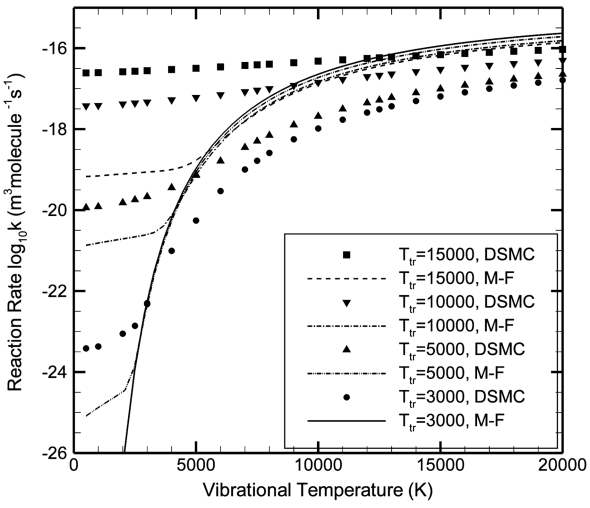

Fig. 20 Oxygen dissociation: DSMC and the M–F model.

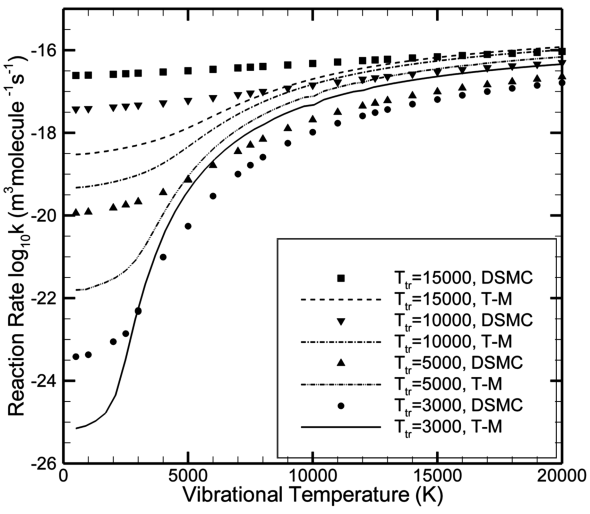

Fig. 21 Oxygen dissociation: DSMC and the T–M model.

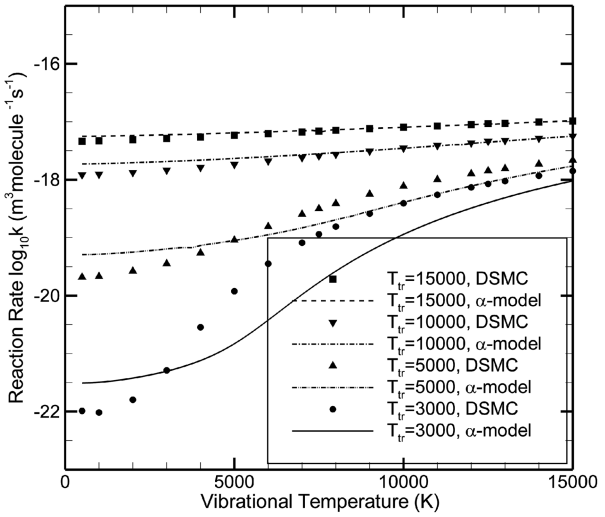

Fig. 22 $N_2 + O \rightarrow NO + N$ exchange reaction. DSMC and the α model.

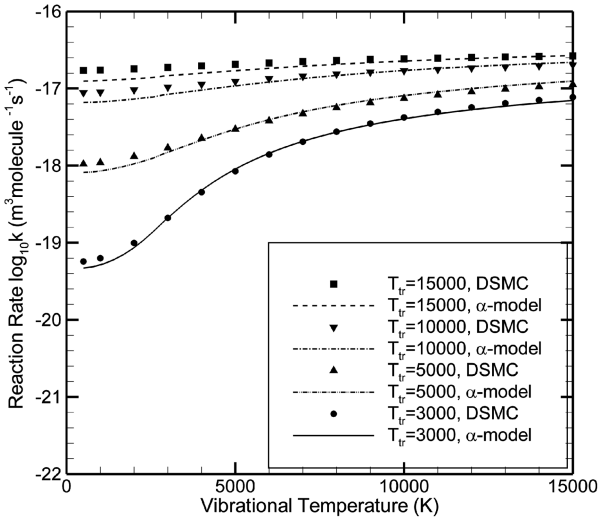

Fig. 23 $NO + O \rightarrow O_2 + N$ exchange reaction: DSMC and the α model.

the energy threshold in addition to the translational energy is judiciously picked and could be related to the average vibrational energy that is disposed to the vibrational mode of the potentially formed products of the reaction. Chernyi et al. [3] gave values of $\alpha = 0.51$ and 0.94 for the reactions in Eqs. (6) and (7) but also point out that α is expected to be in the interval $0.9 \leq \alpha \leq 1.0$ for endothermic reactions. This may be the reason the α model agrees more closely with DSMC for the reaction in Eq. (7), where $\alpha = 0.94$, than for the reaction in Eq. (6), where $\alpha = 0.51$.

The DSMC and α models agree in the low-vibrational-temperature regime, because both models allow the translational energy alone to be used to overcome the energy threshold of the reaction, unlike Park's model, which predicts vanishing reaction rates as the vibrational temperature tends to zero, as observed in the case of dissociation reactions.

D. Comparison of DSMC and Quasi-Classical Trajectory Calculations

In the absence of measured cross sections for reactions between atmospheric species, comparisons can be made to quasi-classical trajectory (QCT) calculations of molecular collisions, where the dependence of the cross section on the energy distribution can be determined accurately. Bose and Candler [23] reported QCT calculations of internal-energy-dependent rates for the endothermic exchange reaction between nitrogen and atomic oxygen of Eq. (6): $N_2 + O \rightarrow NO + N$. They develop an analytical fit of the lowest $^3A'$ potential energy surface based on the contracted configuration interaction ab initio data and use it to obtain the reaction rate from 3000–25,000 K. The QCT equilibrium rates agree with the measured rates, where values are available. Bose and Candler [23] also presented nonequilibrium reaction rates for particular vibrational energy states of molecular nitrogen.

Figure 24 compares the DSMC reaction rates and the QCT rates of Bose and Candler [23] for translational–rotational temperatures of 7000, 10,000, and 14,000 K. In these calculations, all nitrogen molecules are at a particular vibrational level, whereas their translational and rotational energy is distributed according to the equilibrium distribution at the prescribed temperature. The DSMC and QCT values are in fairly good agreement for low temperatures at low-N_2-vibrational levels. However, as the temperature and the vibrational level increase, the difference between the two models increases. The DSMC values appear to be reaching a plateau around vibrational level 12, which is the energy-threshold level of Eq. (4). The reason for this behavior is that the probability of the energy-threshold level appearing in the products increases as the precollisional vibrational energy increases but saturates when the precollisional vibrational energy significantly exceeds the energy-threshold level.

If the condition of Eq. (4) is replaced by the condition

$$i_d \geq i \geq i_a \tag{10}$$

which constrains the energy level of the reactant molecule in a trial redistribution of energy to lie between the energy thresholds of the exchange and dissociation reactions. Figure 24 is replaced by Fig. 25. The DSMC rates based on Eq. (10) are clearly in better agreement with the QCT calculations of Bose and Candler [23] than are the DSMC rates based on Eq. (4). Using the inequality of Eq. (10) as the condition for an endothermic exchange reaction, the equilibrium reaction rate can be analytically determined:

$$k(T) = \frac{2\sigma_{\text{ref}}}{\varepsilon\sqrt{\pi}}\left(\frac{T}{T_{\text{ref}}}\right)^{1-\omega}\left(\frac{2k_B T_{\text{ref}}}{m_r}\right)^{1/2} \times \left(\exp\left[-\frac{i_a\Theta_v}{T}\right] - \exp\left[-\frac{i_d\Theta_v}{T}\right]\right) \tag{11}$$

The second term in the last factor of Eq. (11) becomes important only at high temperatures (greater than 15,000 K). The equilibrium reaction rate for the modified DSMC model [see Eqs. (10) and (11)] is

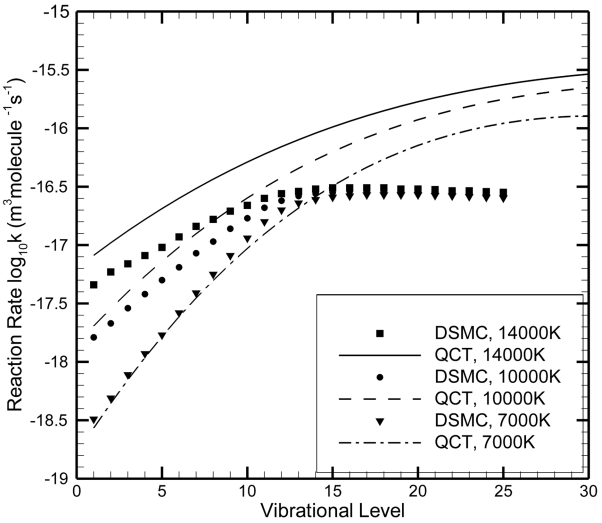

Fig. 24 $N_2 + O \rightarrow NO + N$ exchange reaction: DSMC-Eq. (4) and QCT results.

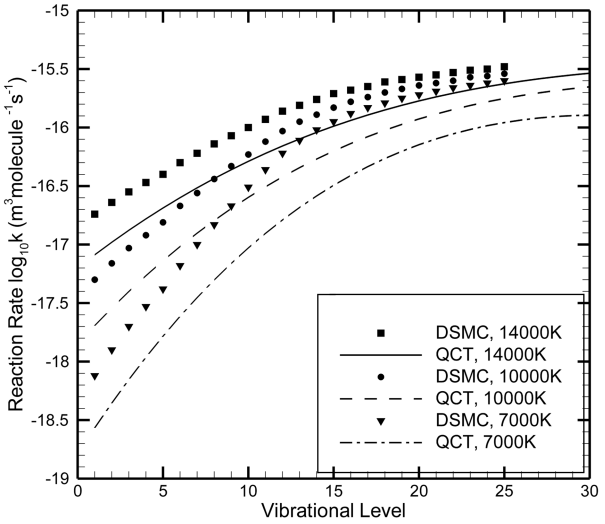

Fig. 25 $N_2 + O \rightarrow NO + N$ exchange reaction: DSMC-Eq. (4) and QCT results.

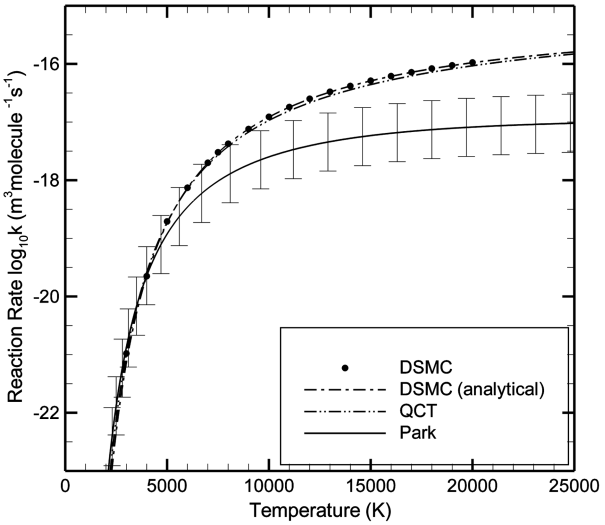

Fig. 26 $N_2 + O \rightarrow NO + N$ exchange reaction: DSMC-Eq. (10), QCT, and Park equilibrium results.

presented in Fig. 26 and is in excellent agreement with the QCT equilibrium reaction rate of Bose and Candler [23].

It is not clear whether Eq. (10) provides a better representation of the actual chemical process than does Eq. (4). As pointed out, the experimental data for this reaction are very limited and have been measured only between 2384–3850 K. Table 1 presents the equilibrium reaction rates of Monat et al. [21], Bose and Candler [23], Park [4], and the DSMC models of Eqs. (4) and (10) at 3000 K, near the middle of the temperature range of the measurements. As expected based on Figs. 24 and 25, Eq. (10) produces somewhat better agreement with the measured rate than does Eq. (4) does.

Table 1 Measured and model rates at 3000 K for $N_2 + O \rightarrow NO + N$

Source	Reaction rate, $\log_{10}(k)$	Difference from Monat et al. [21], %
Monat et al. [21]	−20.94	0
Park [4]	−20.87	16
Bose and Candler [23]	−20.99	11
DSMC/Eq. (4)	−21.30	56
DSMC/Eq. (10)	−21.13	35

V. Conclusions

A recently proposed set of chemical reaction models applicable within the DSMC method has been investigated. The new models, unlike all other DSMC chemical reaction models, do not rely on measured macroscopic reaction rates to determine adjustable parameters. Instead, the new models predict the probability of a chemical reaction occurring during a collision between two molecules based solely on vibrational energy levels and the partition of collisional energy (at present, the models do not account for quantum mechanical effects that constrain transitions between energy states).

Through a series of comparisons, the DSMC models are shown to produce reaction rates in good agreement with Park's suggested reaction rates. The experimental uncertainty of Park's rates does not allow for an unequivocal assessment of the DSMC models through these comparisons. However, the differences between Park's reaction rates and the DSMC values are within one order of magnitude in most cases, which corresponds to the uncertainty estimated by Park for these rates. This degree of agreement observed between the DSMC models and measured and theoretical rates is strong evidence that the DSMC models can provide accurate values for nonequilibrium reaction rates between atmospheric species for hypersonic flows.

For nonequilibrium conditions, the DSMC models produce rates that are in good qualitative and quantitative agreement with theoretical models and that lie within the accuracy of measured nonequilibrium reaction rates. In fact, the DSMC results indicate that, in agreement with theoretical predictions and experimental observations, the selectivity of a reaction rate on the reactant energy diminishes as the total collisional energy increases.

Some differences between Park's model and the DSMC model are observed for low vibrational temperatures. Although the reaction rates are small at these temperatures, the impact of these differences on an actual flow simulation may be significant, as discrepancies between calculated and flight-measured NO concentrations suggest.

Currently, the ability to simulate upper-atmosphere hypersonic flows and environments is hampered by using chemical-reaction-rate models of unknown accuracy that introduce unknown errors into calculations. The new DSMC models may lead to a predictive and self-consistent capability for determining equilibrium and nonequilibrium chemical reaction rates that does not rely on measured equilibrium rates. The new models also simplify validation and uncertainty quantification relative to empirical models because they eliminate the need for adjustable parameters.

Acknowledgments

This work was performed at Sandia National Laboratories. Sandia is a multiprogram laboratory operated by Sandia Corporation, a Lockheed Martin Corporation, for the U.S. Department of Energy's National Nuclear Security Administration under contract DE-AC04-94AL85000.

References

[1] Hammerling, P., Teare, J. D., and Kivel, B., "Theory of Radiation from Luminous Shock Waves in Nitrogen," *Physics of Fluids*, Vol. 2, No. 4, 1959, pp. 422–426. doi:10.1063/1.1724413

[2] Treanor, C. E., and Marrone, P. V., "Effect of Dissociation on the Rate of Vibrational Relaxation," *Physics of Fluids*, Vol. 5, No. 9, 1962, pp. 1022–1026. doi:10.1063/1.1724467

[3] Chernyi, G. G., Losev, S. A., Macheret, S. O., and Potapkin, B. V., *Physical and Chemical Processes in Gas Dynamics: Cross Sections and Rate Constants*, Vol. 1, Progress in Aeronautics and Astronautics, Vol. 197, AIAA, Reston, VA, 2004.

[4] Park, C., *Nonequilibrium Hypersonic Aerothermodynamics*, Wiley, New York, 1990.

[5] Park, C., "Review of Chemical-Kinetic Problems of Future NASA Missions. 1: Earth Entries," *Journal of Thermophysics and Heat Transfer*, Vol. 7, No. 3, 1993, pp. 385–398. doi:10.2514/3.431

[6] Sharma, S. P., Huo, W. M., and Park, C., "The Rate Parameters for Coupled Vibrational-Dissociation in a Generalized SSH Approximation," AIAA Paper 88-2714, 1988.
[7] Gupta, R. N., Yos, J. M., Thompson, R. A., and Lee, K.-P., "A Review of Reaction Rates and Thermodynamics and Transport Properties from an 11-Species Air Model for Chemical and Thermal Nonequilibrium Calculation to 30,000 K," NASA RP-1232, Aug. 1990.
[8] Bird, G. A., *Molecular Gas Dynamics and the Direct Simulation of Gas Flows*, Oxford Univ. Press, Oxford, 1994.
[9] Bird, G. A., "A Comparison of Collision Energy-Based and Temperature-Based Procedures in DSMC," *26th International Symposium on Rarefied Gas Dynamics*, Vol. 1084, edited by T. Abe, American Inst. of Physics, College Park, MD, 2009, pp. 245–250.
[10] Gallis, M. A., Bond, R. B., and Torczynski, J. R., "A Kinetic-Theory Approach for Computing Chemical-Reaction Rates in Upper-Atmosphere Hypersonic Flows," *Journal of Chemical Physics*, Vol. 131, 2009, Paper 124311. doi:10.1063/1.3241133
[11] Hirschfelder, J. O., Curtiss, C. F., and Bird, R. B., *Molecular Theory of Gases and Liquids*, Wiley, New York, 1954.
[12] Wagner, W. A., "Convergence Proof for Bird's Direct Simulation Monte Carlo Method for the Boltzmann Equation," *Journal of Statistical Physics*, Vol. 66, Nos. 3–4, 1992, pp. 1011–1044. doi:10.1007/BF01055714
[13] Gallis, M. A., Torczynski, J. R., and Rader, D. J., "Molecular Gas Dynamics Observations of Chapman–Enskog Behavior and Departures Therefrom in Nonequilibrium Gases," *Physical Review E (Statistical Physics, Plasmas, Fluids, and Related Interdisciplinary Topics)*, Vol. 69, No. 4, 2004, Paper 042201. doi:10.1103/PhysRevE.69.042201
[14] Gallis, M. A., Torczynski, J. R., Rader, D. J., Tij, M., and Santos, A., "Normal Solutions of the Boltzmann Equation for Highly Non-equilibrium Fourier and Couette Flow," *Physics of Fluids*, Vol. 18, Jan. 2006, Paper 017104. doi:10.1063/1.2166449
[15] Gallis, M. A., and Harvey, J. K., "Modeling of Chemical Reactions in Hypersonic Rarefied Flow with DSMC," *Journal of Fluid Mechanics*, Vol. 312, 1996, pp. 149–172. doi:10.1017/S0022112096001954
[16] Wadsworth, D. C., and Wysong, I. J., "Vibrational Favoring Effect in DSMC Dissociation Models," *Physics of Fluids*, Vol. 9, No. 12, 1997, pp. 3873–3884. doi:10.1063/1.869487
[17] Gallis, M. A., and Harvey, J. K., "On the Modeling of Thermochemical Nonequilibrium in Particle Simulations," *Physics of Fluids*, Vol. 10, No. 6, 1998, pp. 1344–1358. doi:10.1063/1.869660
[18] Dressler, R. A., *Chemical Dynamics in Extreme Environments*, World Scientific, Hackensack, NJ, 2001.
[19] Wysong, I. J., Dressler, R. A., Chiu, Y. H., and Boyd, I. D., "Direct Simulation Monte Carlo Dissociation Model Evaluation: Comparison to Measured Cross Sections," *Journal of Thermophysics and Heat Transfer*, Vol. 16, No. 1, 2002, pp. 83–93. doi:10.2514/2.6655
[20] Lord, R. G., "Modeling Vibrational Energy Exchange of Diatomic Molecules Using the Morse Interatomic Potential," *Physics of Fluids*, Vol. 10, No. 3, 1998, pp. 742–746. doi:10.1063/1.869598
[21] Monat, J. P., Hanson, R. K., and Kruger, C. H., "Shock Tube Determination of the Rate Coefficient for the Reaction $N_2 + O \rightarrow NO + N$," *Proceedings of the 17th Symposium (International) on Combustion*, Combustion Inst., Pittsburgh, PA, 1978, pp. 543–552.
[22] Levine, R. D., and Bernstein, R. B., *Molecular Reaction Dynamics and Chemical Reactivity*, Oxford Univ. Press, Oxford, 1988.
[23] Bose, D., and Candler, G. V., "Thermal Rate Constants of the Reaction Using Ab Initio Potential Energy Surfaces," *Journal of Chemical Physics*, Vol. 104, No. 8, 1996, pp. 2825–2833. doi:10.1063/1.471106
[24] Sergievskaya, A. L., Kovach, E. A., Losev, S. A., and Kuznetsov, N. M., "Thermal Nonequilibrium Models for Dissociation and Chemical Exchange Reactions at High Temperatures," AIAA Paper 96-1895, 1996.
[25] Pogosbekian, M. Ju., Sergievskaya, A. L., and Losev, S. A., "Verification of Theoretical Models of Chemical Exchange Reactions on the Basis of Quasi-Classical Trajectory Calculations," *Chemical Physics*, Vol. 328, Nos. 1–3, 2006, pp. 371–378. doi:10.1016/j.chemphys.2006.07.027
[26] Capitelli, M., Esposito, F., Kustova, E. V., and Nagnibeda, E. A., "Rate Coefficients for the Reactions $N_2(i) + N = 3N$: A Comparison of Trajectory Calculations and the Treanor–Marrone Model," *Chemical Physics Letters*, Vol. 330, Nos. 1–3, 2000, pp. 207–211. doi:10.1016/S0009-2614(00)00954-4